TEST RESULTS ON RF ACCELERATING CAVITIES FOR THE POSITRON DAMPING RING AT SuperKEKB

Tetsuo Abe*, Yasunao Takeuchi, Tatsuya Kageyama, Hiroshi Sakai, Kazuo Yoshino,
KEK, Tsukuba, Ibaraki 305-0801, Japan

Abstract

A positron damping ring (DR) has been constructed to fulfill the requirement for the low-emittance positron-beam injection into the main ring (MR) of SuperKEKB which is based on the nano-beam scheme [6]. We have proposed and developed a radio-frequency (RF) accelerating structure for the DR, which can supply 2.4 MV accelerating voltage at maximum with three cavities to be installed in a limited space. In fiscal 2013, we constructed the second production-version cavity (cavity No.2) based on the developments of the prototype cavity (prototype) and the first production-version cavity (cavity No.1). In this paper, we present results of low-power and high-power tests of cavity No.2, compared with the results of the prototype and cavity No.1, and show also results of advanced studies on the high power test of cavity No.2.

INTRODUCTION

A DR has been constructed to fulfill the requirement for the low-emittance positron-beam injection into the MR of SuperKEKB which is based on the nano-beam scheme. For the DR, we have proposed an RF accelerating structure as shown in Fig. 1 [1], and developed an RF cavity (DR cavity) as shown in Fig. 2a [2]. We designed the DR cavity based on the higher-order-mode (HOM) damped structure of the normal-conducting (NC) RF accelerating cavity system ARES [3] (hereinafter simply referred to as "the ARES") because highly-stable operation is required for the DR cavities, and we have successful experiences of the long-term operation of 32 cavities of the ARES at the KEKB MRs with extremely low trip rates (< 1/cavity/(90 days)).

Since the RF operation frequency is the same as used for the MRs, which is 508.887 MHz, the basic structure of the DR cavity is the same as that of the accelerating cavity in the ARES. We chose the accelerating voltage per cavity (cavity voltage (V_c)) in specification to be 0.8 MV, higher than that of the ARES (0.5 MV). The details on this accelerating structure for the DR are described in [6].

We constructed the prototype in fiscal 2011, and performed a high power test in fiscal 2012. Using the results of the prototype, we constructed cavity No.1 in fiscal 2012, and performed a high power test in fiscal 2013. We also constructed cavity No.2 (Fig. 2b) in fiscal 2013, and performed a high power test from May 12 to July 4 of fiscal 2014. In this paper, we present results of low-power and high-power tests of cavity No.2, compared with the results of the prototype and cavity No.1, and show also results of advanced studies on the high power test of cavity No.2.

* tetsuo.abe@kek.jp

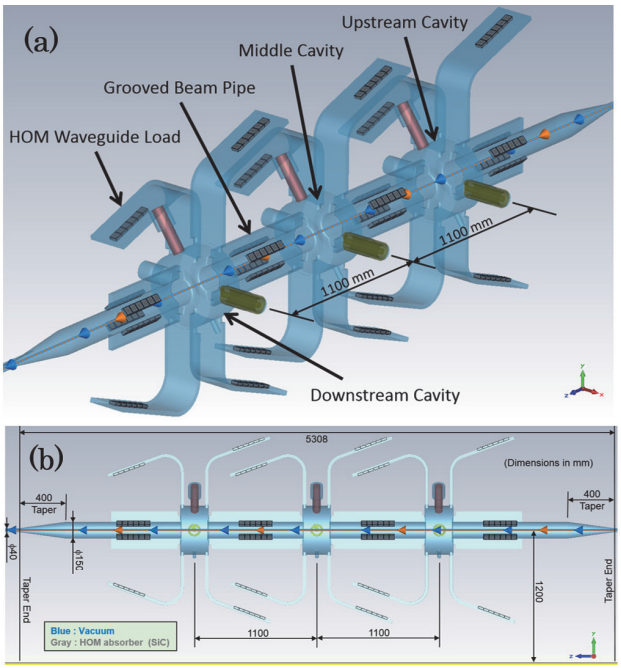

Figure 1: Overview of the RF accelerating structure for the SuperKEKB positron damping ring. The colored arrows indicate the direction of the positron beam. The blue (gray) region indicates the vacuum (HOM absorbers made of SiC ceramics). (a) Perspective view. (b) Side view.

DR CAVITY

The basic structures are the same among the prototype, cavity No.1, and No.2, where the conceptual diagram is shown in Fig. 2a. Table 1 shows design parameters of cavity No.1 and No.2.

Table 1: Design parameters of the DR cavity

Frequency	508.887	MHz
R_{sh}/Q_0	150	Ω
Q_0	≈ 30000	
Cavity Voltage	0.8	MV
Wall-Loss Power	≈ 140	kW

The main body of the DR cavity is made of high-purity oxygen-free copper (class1), and consists of a barrel and two discoid endplates. The barrel and two endplates were machined with an accuracy of 50 μm and 3S surface roughness, then bonded into a cavity in the final brazing. For the purpose of frequency tuning, one of the endplates has a bump with an initial height of 2.5 mm (tuning bump) in the surface region with high magnetic field applied during

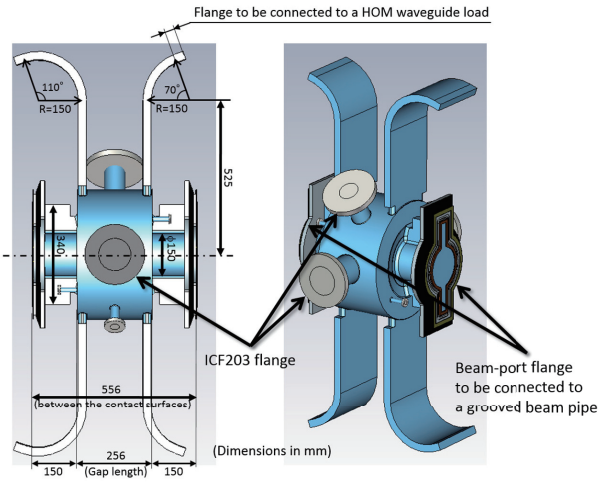

(a) Conceptual diagram of the main body of the DR cavity (single cell). The blue region indicates the vacuum. The gap length of this cavity is 256 mm.

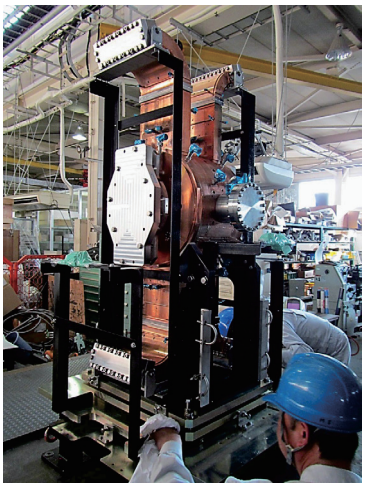

(b) Cavity No.2 just after delivery

Figure 2: DR cavity.

high power operation. The endplate with (without) such tuning bump is called tuning endplate (TEP) (fixed endplate (FEP)). The FEP and TEP are located upstream and downstream of the barrel with respect to the positron beam direction, respectively.

The fabrication method is the same between cavity No.1 and No.2; however, in the final brazing of the cavity, a part of brazing filler metal (BAg-8) squirted from between the barrel and TEP into the inside of cavity No.2, which did not occurred for cavity No.1. Therefore, before the delivery, we performed baking of cavity No.2 for 15 hours with keeping a ribbon-heater temperature of 100 degC [5], where the ribbon heaters were wrapped around the joints between the barrel and endplates, while no baking was applied to cavity No.1. Then, we confirmed the followings before, after, and during the baking with a vacuum pressure lower than 3.5×10^{-5} Pa:

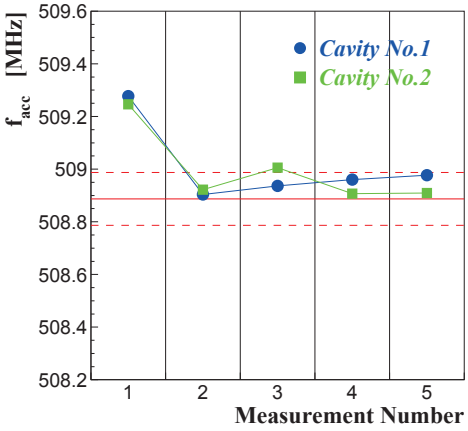

Figure 3: Measurements of the accelerating-mode frequency (f_{acc}), converted to those for a cavity temperature of 30 degC and vacuum inside the cavity, with the movable tuner at its home position (15 mm inside). The horizontal solid and dashed lines indicate a target frequency and its range (±100 kHz), respectively. The measurement number indicates each step in the production process, 1: before the frequency tuning (with air inside), 2: after the frequency tuning and before the final brazing (with air inside), 3: after the final brazing and before the delivery (with air inside), 4: during the preparation for the high power test at the test stand (with nitrogen inside), and 5: just before the start of the high power test (with vacuum inside).

- No gas components observed using a Q-mass spectrometer other than those observed for cavity No.1, and
- No vacuum-pressure spikes or abnormal increases.

Finally, cavity No.2 has passed a usual vacuum leak test with a background level lower than 1.3×10^{-10} Pa m^3/s.

LOW POWER TEST

Before the high power tests, we checked the RF performance of the cavities with low RF power. Measured values shown in this section were obtained by one-port measurement through the input coupler (reuse from KEKB [4]) using a network analyzer, where the measurement method and setup are the same among the prototype, cavity No.1 and No2.

Accelerating-Mode Frequency (f_{acc})

Accelerating-mode (TM_{010}) frequency is one of the most important quantities for RF cavities. Figure 3 shows the history of the measured frequency of cavity No.2 together with that of cavity No.1. Only the frequency of cavity No.2 after the final brazing before the delivery is outside the specification, about 120 kHz higher than the target; the reason has not yet been understood, however, it is likely a mismeasurement. Finally, we have achieved and established 0.02 % accuracy in the frequency.

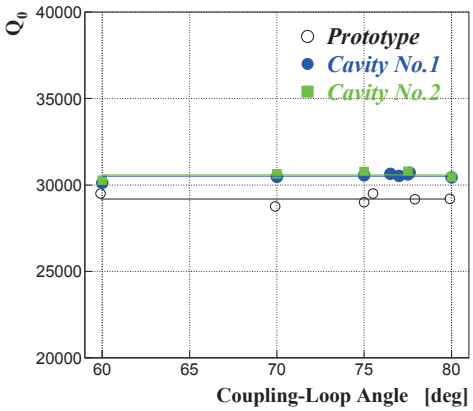

Figure 4: Measurements of Q_0 for the prototype (open circles), cavity No.1 (closed circles), and No.2 (closed squares), converted to those with a cavity temperature of 20 degC. Fitting these measurements with a constant, the Q_0 values are estimated to be 29186 (92.9%IACS) for the prototype, 30506 (97.1%IACS) for cavity No.1, and 30586 (97.3%IACS) for cavity No.2. Reduced χ^2 values in the fittings, assuming a 0.5 % error for Q_0, are all smaller than 1.0.

Unloaded Quality Factor (Q_0)

Q_0 is also an important quantity for RF cavities. Figure 4 shows Q_0 measurements as a function of the coupling loop angle of the input coupler. Fitting the measurements with a constant, the Q_0 values are estimated to be 92.9 %IACS for the prototype, 97.1 %IACS for cavity No.1, and 97.3 %IACS for cavity No.2. The Q_0 values of cavity No.1 and No.2 is about 4 % higher than that of the prototype. This difference can be attributed to a difference of the surface protection process for the surfaces of the endplates to be exposed to high RF fields: acid cleaning followed by chromating applied to the prototype, while electro-polishing (EP) with about 40 μm of etching applied to cavity No.1 and No.2 instead [7]. This Q_0 improvement is consistent with the improvement of the surface roughness on the endplates by EP. Comparing the Q_0 values between cavity No.1 and No.2, no effect of the squirt of the brazing filler metal on cavity No.2 is seen in low-power Q_0.

External Quality Factor (Q_{ext})

We also measured $Q_{\rm ext}$ on the input coupler as a function of the coupling-loop angle, and adjusted the angle so that the input coupler was slightly over-coupled. The coupling factors for the high power tests of the prototype, cavity No.1 and No2, measured with low RF power, were all in a range from 1.31 to 1.34 for a cavity temperature of 30 degC.

HIGH POWER TESTS

The setup of the high power test for cavity No.2 is shown in Fig. 5, which is the same as that for cavity No.1 [7] except for mirror chambers (shown in Fig. 6) [8] attached to the beam-port flanges. Near the beam axis, radiation level is high during high power operation, so that a mirror is located inside the mirror chamber to view the inside of the cavity. Then, we attach a TV camera to the view port of the chamber far from the beam axis. For cavity No.1, we used only one mirror chamber with a circular mirror, while for cavity No.2, two mirror chambers with elliptical mirrors in order to have a wider view. In total, we used three TV cameras as shown in Fig. 5 (TV camera 1, 2, and 3) for cavity No.2, and the videos were recorded in the NTSC format with a frame rate of 29.97 fps.

We first fed high RF power into the cavity with keeping the vacuum pressure lower than a specified value (reference vacuum pressure shown in Fig. 7 with light blue lines), by an automatic computer control, toward V_c = 0.95 MV, where V_c = 0.95 MV is the highest voltage permitted by the radiation regulation for this test stand. After reaching V_c = 0.95 MV, we performed a stability test with keeping a constant cavity voltage. The former is hereinafter referred to as conditioning period, and the latter one as stability-test period.

Conditioning Period

Figure 7b shows the conditioning history of cavity No.2, where V_c reached 0.90 MV (0.95 MV) without any problems in 95 (107) hours, exceeding the cavity voltage required by the specifications (0.8 MV), where V_c is calculated according to the formulae described in [6, 7].

Also shown in Fig. 7a is the conditioning history of cavity No.1 for comparison, where V_c reached 0.90 MV in 83 hours, and only data with $V_c \leq$ 0.90 MV are plotted here because data with $V_c >$ 0.90 MV is included in the stability-test period in the case of cavity No.1. It could be said that the conditioning speed of cavity No.2 is comparable to that of cavity No.1.

Stability-Test Period

After reaching V_c = 0.95 MV, we performed a stability test of cavity No.2 for 16 days with the following sequence each day:

1. Powering and stepping up the cavity voltage up to 0.94 or 0.95 MV in the morning.
2. Keeping the cavity voltage for 30 minutes.
3. Stepping down to V_c = 0.90 MV.
4. Keeping V_c = 0.90 MV until 17:00 in the evening.

Finally, we kept V_c = 0.90 MV for 80 hours of integrated time. During the 80 hours, eleven cavity breakdowns occurred, where the definition of cavity breakdown is described in Appendix. This number of cavity breakdowns is equivalent to a cavity breakdown rate of $3.3^{+1.3}_{-1.0}$ / day for cavity No.2, where an statistical error is shown according to Poisson statistics. This cavity breakdown rate at V_c = 0.90 MV is consistent with that of cavity No.1: $5.0^{+4.8}_{-2.7}$ / day, obtained in the same manner [7].

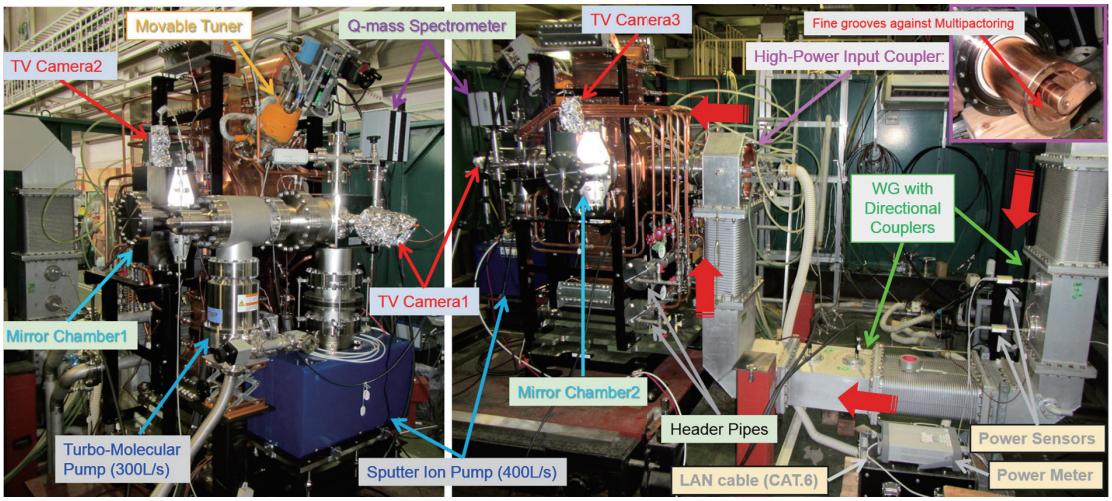

Figure 5: Setup of the high power test for cavity No.2 at the test stand in the radiation controlled area. The red arrows indicate the flow of the high RF power coming from a 1 MW CW klystron. The flow rate of the cooling water for the cavity was about 130 L/min, where the temperature of the input water was 30 degC.

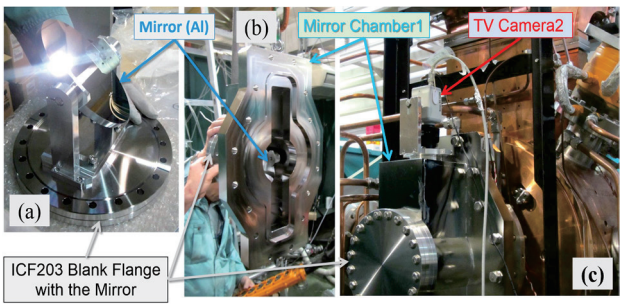

Figure 6: Mirror chamber used for the high power test of cavity No.2. (a) Elliptical mirror (Al) mounted on an ICF203 blank flange. (b) Vacuum chamber (SUS304) containing the mirror, whose inner surface was electro-polished. (c) The mirror chamber is attached to cavity No.2.

DATA ANALYSES

We have performed advanced studies on the high power test for cavity No.2.

Classification and Statistics of Cavity-Trip Events

In this paper, cavity trip is defined as an event during high power operation when the interlock system works due to a reason related to the cavity. Cavity-trip events are classified into three:

1. Events with a vacuum pressure rise over a threshold in a range from 4.1×10^{-5} to 1.0×10^{-4} Pa depending on the base pressure (hereinafter referred to as cavity-vacuum events),
2. Cavity-breakdown events, and
3. Others.

It should be noted that cavity-breakdown events with a vacuum pressure rise over the threshold are not included in the class of cavity vacuum. Table 2 shows the classification and number of the cavity-trip events, which means that almost all the events are cavity breakdowns.

Table 2: Classification and number of the cavity-trip events. "Vac." and "BD" mean cavity vacuum and cavity breakdown, respectively.

Period	Vac.	BD	Others
Conditioning	2	180	1
Stability test (total)	0	25	0
Stability test (V_c = 0.90 MV)	0	11	0

Table 3 shows number of cavity-breakdown events with any abnormality observed in the videos at a moment when the interlock system worked, together with proportions to the total number of the cavity-breakdown events, created by checking carefully every frame of the videos. In any period, such proportion is about 80 %, and this large proportion means that most of the cavity-breakdown events have signals observable with the TV camera(s).

Table 3: Number of cavity-breakdown events with any abnormality observed with any of the three TV cameras. The numbers enclosed in square brackets are proportions to the total number of the cavity-breakdown events.

Period	Abnormality observed
Conditioning	143 [79.4%]
Stability test (total)	20 [80.0%]
Stability test (V_c = 0.90 MV)	9 [81.8%]

Table 4 shows breakout of the cavity-breakdown events, where an event with a "Spot-type explosion with a BS" is defined as a cavity-breakdown event with a rapid increase of light intensity of a bright spot (BS) at the moment of the breakdown. Figure 8 shows an example of such events, where the BS on the FEP at 3 o'clock exploded and disappeared.

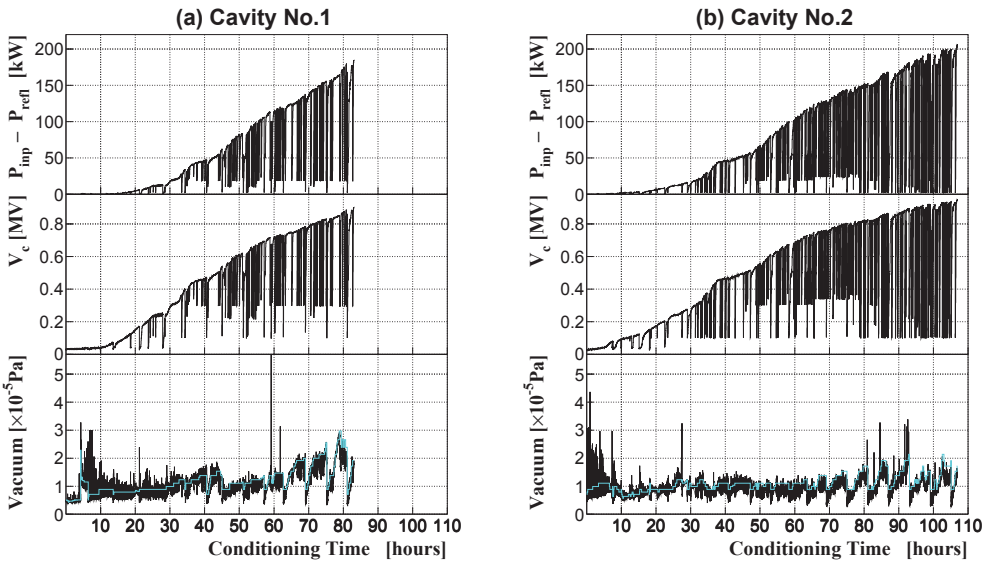

Figure 7: Conditioning histories until V_c reached 0.95 MV (0.90 MV) with data points recorded every ten seconds plotted for cavity No.2 (No.1). Data with holding the input RF power (P_{inp}) and data for tuning the control system or klystron are excluded here. P_{refl} indicates the reflected RF power from the cavity. The light blue lines indicate the reference vacuum pressure specified in the automatic conditioning by computer control. If the vacuum pressure is higher than the reference, the power is slightly stepped down until the vacuum pressure becomes lower than the reference, and then the power is slightly stepped up as long as the vacuum pressure is lower than the reference.

Table 4: Breakout of the cavity-breakdown events. The numbers enclosed in square brackets (parentheses) indicate proportions to the cavity-breakdown events (events with any abnormality observed).

Period	Spot-type explosion with a BS	Spot-type explosion without any BS	Non-spot-type flash	Non-spot-type lightning(s) only	Others
Conditioning	44	72	4	14	9
	[24.4%] (30.8%)	[40.0%] (50.3%)	[2.2%] (2.8%)	[7.8%] (9.8%)	[5.0%] (6.3%)
Stability test (total)	7	9	3	1	0
	[28.0%] (35.0%)	[36.0%] (45.0%)	[12.0%] (15.0%)	[4.0%] (5.0%)	
Stability test	5	2	1	1	0
(V_c = 0.90 MV)	[45.5%] (55.6%)	[18.2%] (22.2%)	[9.1%] (11.1%)	[9.1%] (11.1%)	

Table 5 shows number of cavity-breakdown events with BSs exploded and disappeared, showing that almost all the BSs disappeared after the explosions, and this kind of phenomenon is a significant component of the cavity conditioning (at least 25 % of the cavity-breakdown events).

Figure 9 (Figure 10) shows snapshots of the FEP (TEP) in the case of V_c = 0.90 MV, respectively, in chronological order. It is clearly seen that the number of BSs had been decreasing although some BSs had become brighter, and there appeared a few new BSs.

In Tab. 4, an event with a "Spot-type explosion without any BS" is defined as a cavity-breakdown event with a spot-type explosion, where there is no BS there, which continues to be bright and visible for at least 2 seconds just before the explosion. It should be particularly noted that, in several percent of such events, a BS suddenly appeared at a position of the explosion in a time range of the last 2 seconds before the cavity breakdown. Figure 11 (Table 6) shows an example (the number) of such events. In such events, there

Table 5: Number of spot-type explosion events with BSs, where the BSs disappeared after the explosions. The numbers enclosed in square brackets (parentheses) indicate proportions to the total number of the cavity-breakdown events (events with any abnormality observed).

Period	BS disappeared
Conditioning	36
	[20.0%] (25.2%)
Stability test (total)	7
	[28.0%] (35.0%)
Stability test (V_c = 0.90 MV)	5
	[45.5%] (55.6%)

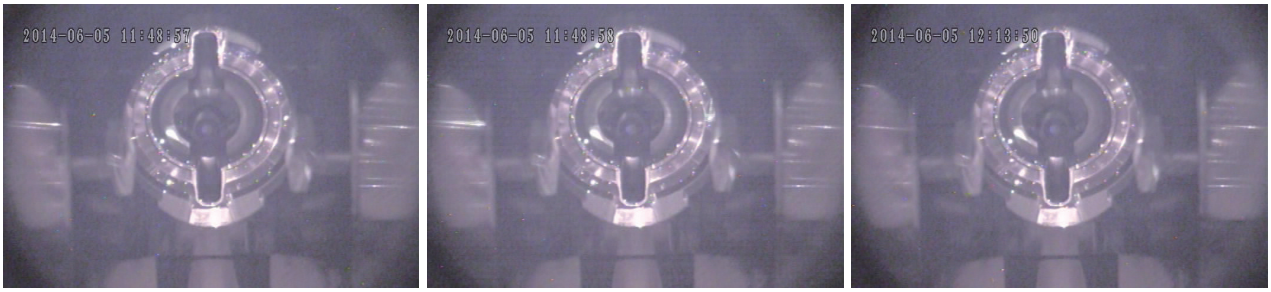

(a) $T = -0.03$ seconds. (b) $T = 0$. (c) $T > 0$.

Figure 8: Example of the spot-type explosion events with BSs. Snapshots of the FEP, recorded with the TV camera 3, are shown in chronological order. The BS at 3 o'clock exploded and disappeared. $V_c = 0.95$ MV.

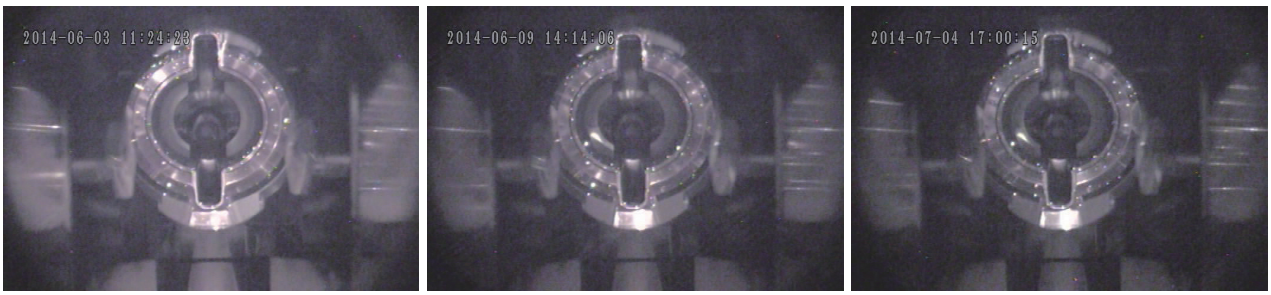

(a) During the conditioning. (b) A day before starting the stability test. (c) At the end of the stability test.

Figure 9: Snapshots of the FEP, recorded with the TV camera 3, in the case of $V_c = 0.90$ MV.

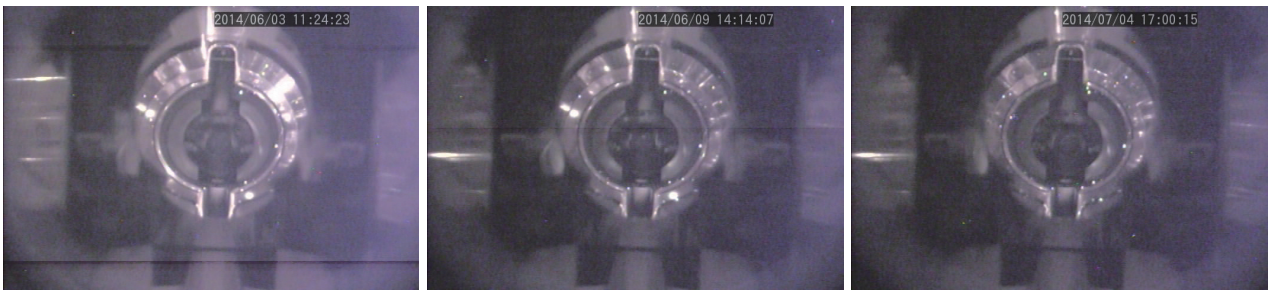

(a) During the conditioning. (b) A day before starting the stability test. (c) At the end of the stability test.

Figure 10: Snapshots of the TEP, recorded with the TV camera 2, in the case of $V_c = 0.90$ MV.

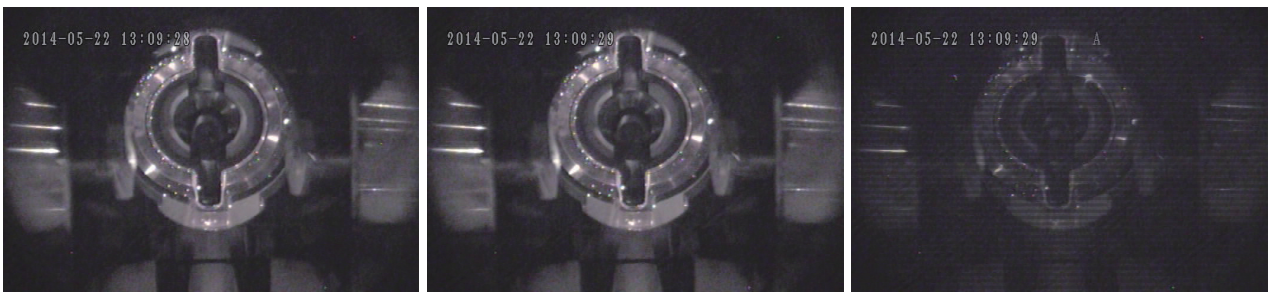

(a) 2 frames before the cavity breakdown. (b) 1 frame before the cavity breakdown. (c) At the moment of the cavity breakdown.

Figure 11: Snapshots of the FEP, recorded with the TV camera 3, showing a spot-type explosion with a sudden BS appearance and explosion at 1 o'clock. $V_c = 0.56$ MV.

was relevant microscopic dynamics: generation, growth, and explosion of BSs, and then breakdowns, in a time scale of the order of 0.1 s or shorter. We could make a possible hypothesis that there is a common mechanism including the above process in all of the spot-type explosion events without any BS, and this kind of phenomenon is also a significant component of cavity conditioning (at least 40 % of the cavity-breakdown events).

Table 6: Number of cavity-breakdown events with sudden BS appearance. The numbers enclosed in square brackets (parentheses) indicate proportions to the total number of the cavity-breakdown events (events with any abnormality observed).

Period	Sudden BS appearance
Conditioning	6
	[3.3%] (4.2%)
Stability test (total)	0
Stability test (V_c = 0.90 MV)	0

Figure 12 shows distributions of the spot positions, on the endplates, of the spot-type explosion events (132 points in total, sum of the second and third columns of Tab. 4). The surface electromagnetic field is shown in Fig. 13 for reference together with regions observable with the TV camera 2 or 3 shown with white dashed ellipses. A clear non-uniformity is found, in Fig. 12, in the azimuthal direction, which should be attributed to some cavity production process(es); however, no clear correlation has been found so far. Further investigation is ongoing because results should help us to have better performance of future RF cavities.

Figure 14 shows examples of the non-spot-type events, where it is difficult to identify spots.

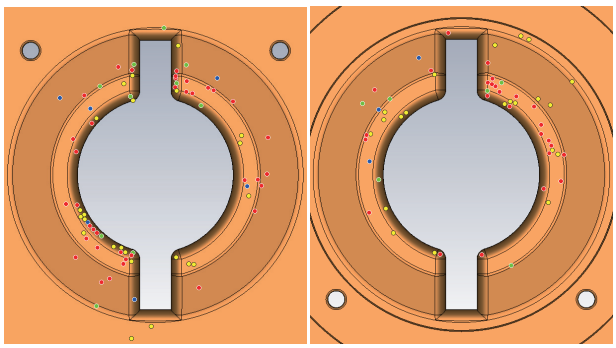

(a) FEP. (b) TEP.

Figure 12: Spot-position distributions of the spot-type explosion events. The plot colors of blue, green, yellow, and red indicate cavity-voltage ranges of $V_c \leq 0.40$ MV, $0.40 < V_c \leq 0.60$ MV, $0.60 < V_c \leq 0.80$ MV, and $0.80 < V_c \leq 0.95$ MV, respectively. The small holes are monitor ports for pickup antennas.

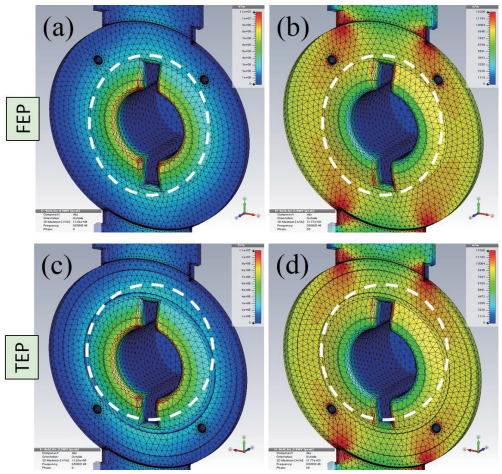

Figure 13: Surface-field strengths for V_c = 0.90 MV together with the curved tetrahedral meshes used to estimate the theoretical Q_0 and frequency. The regions inside the white dashed ellipses are observable with the TV camera 2 or 3 shown in Fig. 5. (a) Electric field strength on the FEP, (b) Magnetic field strength on the FEP, (c) Electric field strength on the TEP, and (d) Magnetic field strength on the TEP. The maximum electric surface field strength is 13.3 MV/m for V_c = 0.90 MV.

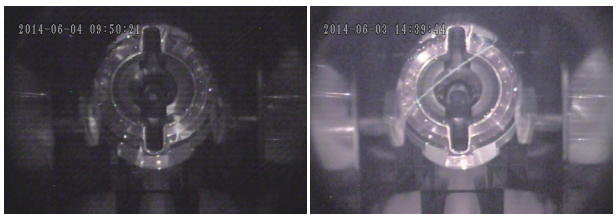

(a) With flash. (b) With lightning only.

Figure 14: Examples of the non-spot-type events with V_c = 0.56 MV. The left (right) example is included in the fourth (fifth) column of Tab. 4.

Outgassing at cavity trips

There were only two cavity-vacuum events. The first (second) event has a vacuum pressure rise (ΔP) of $\Delta P = 3.7 \times 10^{-5} - 1.7 \times 10^{-5} = 2.0 \times 10^{-5}$ Pa ($\Delta P = 8.0 \times 10^{-5} - 9.3 \times 10^{-6} = 7.1 \times 10^{-5}$ Pa) with V_c = 0.258 MV (V_c = 0.463 MV), based on the data recorded every 0.1 s.

Cavity-breakdown events have also vacuum-pressure rises, as shown in Fig. 15. Most of the ΔP values are lower than 5×10^{-6} Pa, however, some events have vacuum-pressure rises comparable to those of the cavity-vacuum events ($> 1 \times 10^{-5}$ Pa), where the maximum ΔP is 5.1×10^{-5} Pa. Such high vacuum-pressure rises are concentrated late the conditioning period near V_c = 0.95 MV as shown in Fig. 15a. In the other periods, the vacuum pressure rises are of the order of 10^{-6} Pa, especially in the stability-test period with V_c = 0.90 MV.

Figure 17 shows partial vacuum-pressure rises at the cavity breakdowns during the stability test, measured using the Q-mass spectrometer. Carbon-based gases (CO and CO_2)

are dominant in most of the events, and hydrogen gas is visible in some events, and not in the other events.

Field Emission

Field emission from the inner surfaces of the endplates leads to generation of X-rays when field-emitted electrons accelerate and impact on opposite inner surface. Therefore, field emission can be seen as an increase of the radiation dose rate near the cavity, higher than the background level. Figure 16a shows radiation dose rates measured near the prototype, cavity No.1, and No.2. The radiation dose rates of cavity No.1 and No.2 in a V_c range from 0.825 to 0.850 MV are about one fifth of that of the prototype, which is one of the results of EP. Figure 16b shows radiation dose rates at V_c = 0.90 MV as a function of day; the field emission became lower during the conditioning period, however, almost constant during the stability test. This fact is consistent with the data shown in Fig. 16a (magenta squares and green squares); the field emission became the minimum level at the end of the conditioning.

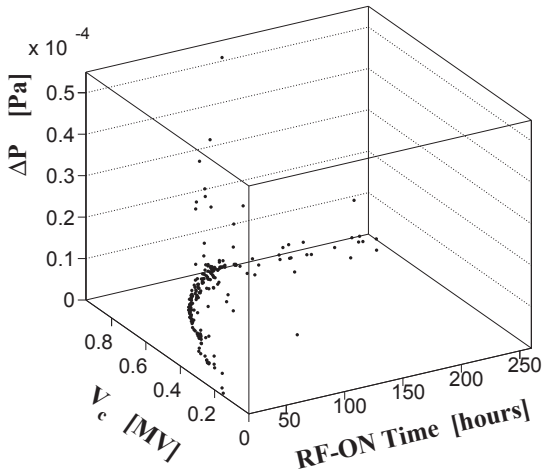

(a) As functions of V_c and RF-ON time.

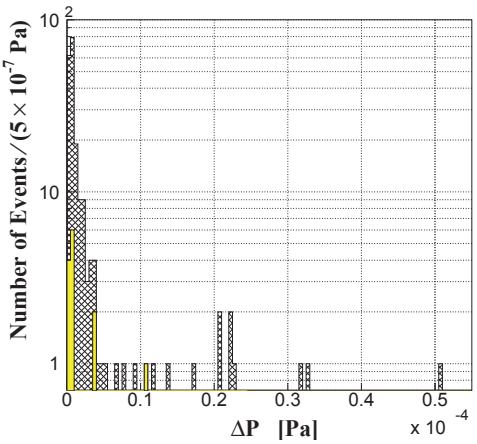

(b) The hatched histogram is on ΔP, equivalent to a projection of (a) to the axis of ΔP. The yellow filled histogram is a part of the hatched histogram, containing the stability test data with V_c = 0.90 MV only.

Figure 15: Vacuum-pressure rises at the cavity breakdowns. The period with RF-ON times before 144 hours is for the conditioning, and the period after 144 hours is for the stability test

SUMMARY AND CONCLUSIONS

We have constructed and tested cavity No.2 for the positron damping ring at SuperKEKB, and demonstrated the RF performance to be equivalent to that of cavity No.1, so that cavity No.2 is also usable for DR operation.

We have performed advanced studies on the high power test of cavity No.2, and experimentally found the following facts, by the direct observation of the inside of the cavity,

- At least 65 % of the cavity-breakdown events are spot-type,
- At moments of at least 20 % of the cavity-breakdown events, BSs exploded, and then disappeared,

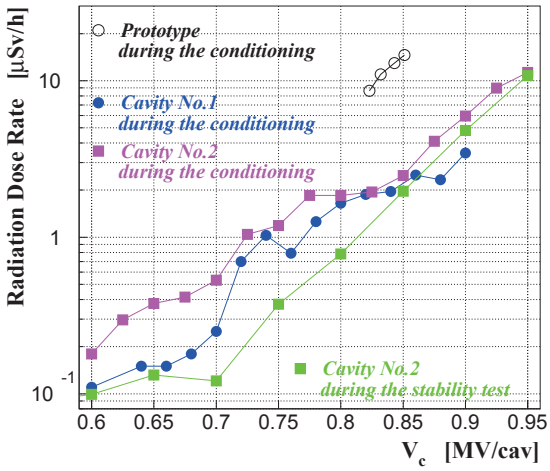

(a) As a function of V_c.

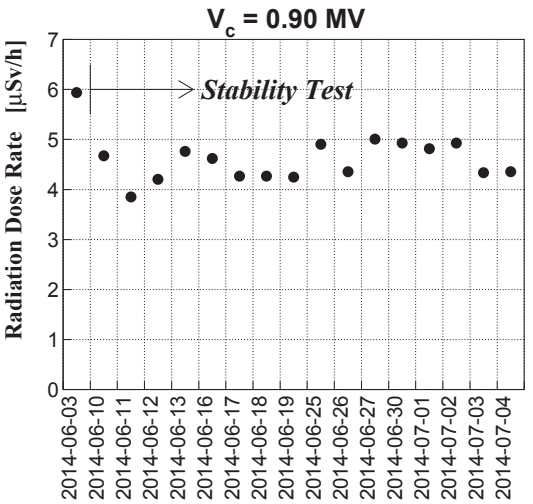

(b) As a function of time (day).

Figure 16: Radiation dose rates measured at about 2 m away from the cavities in the radiation controlled area. The background level is about 0.1 μSv/h.

- In 3 % of the cavity-breakdown events, we observed sudden appearance of BSs in a time range of the last 2 seconds before the explosions and breakdowns, and
- The spot positions are around the nose cone with high electric surface field,

and then, by using the Q-mass spectrometer and radiation detector,

- Some of the cavity-breakdown events have significant vacuum-pressure rises, where carbon-based gases (CO and CO_2) are dominant components of emitted gases,
- The radiation from the cavity decreased during the conditioning period, while it was constant during the stability test,

respectively. The above facts can be important inputs to understanding of breakdown mechanism in NC RF cavities, and should help us to have better performance of future RF cavities.

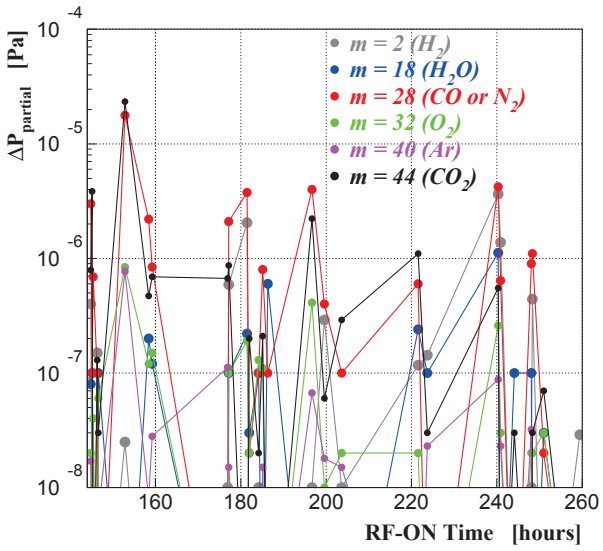

Figure 17: Partial vacuum-pressure rises ($\Delta P_{\mathrm{partial}}$) at the cavity breakdowns, measured using the Q-mass spectrometer shown in Fig.5 every one second, for mass numbers of 2, 18, 28, 32, 40, and 44 as a function of the RF-ON time during the stability test.

APPENDIX

Cavity breakdown is identified if the interlock system works with the reflected RF power over a specified threshold, and the pickup signal from the cavity decays much faster than the decay time constant ($\approx 8\,\mu$s) of the loaded quality factor (≈ 13000). Here, the threshold was in a range from 16 to 28 kW depending on the actual reflected RF power ($\lesssim$ 3 kW for $V_c \leq 0.95$ MV), Figure 18a shows an example of events when the interlock system worked due to a reason not related to the cavity, where such decay time constant is seen in the pickup signal from the cavity. On the other hand, Fig. 18b shows an example of the cavity-breakdown events, where the pickup signal decayed faster than 1 μs.

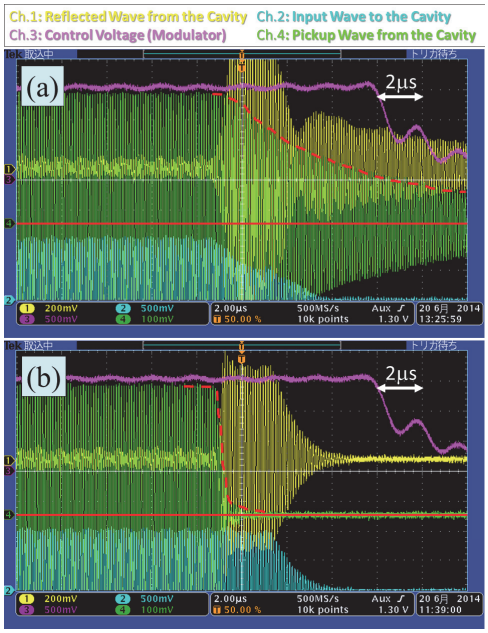

Figure 18: Waveforms of the oscilloscope displayed with a time span of 20 μs (2 μs/div). The red dashed curves indicate the envelope of the pickup wave from cavity No.2, and the red solid lines indicate the zero amplitude. (a) When the RF switch was turned off due to a reason related to the klystron. (b) Example of the cavity-breakdown events.

REFERENCES

[1] T. Abe, T. Kageyama, H. Sakai, Y. Takeuchi, and K. Yoshino, in Proceedings of the 8th Annual Meeting of Particle Accelerator Society of Japan, August 2011 (Paper ID: TUPS131).

[2] T. Abe, T. Kageyama, H. Sakai, Y. Takeuchi, and K. Yoshino, in Proceedings of the 9th Annual Meeting of Particle Accelerator Society of Japan, Aug. 2012 (Paper ID: THLR06).

[3] T. Kageyama, et al., KEK Preprint No. 98-45, 1998.

[4] F. Naito, et al., KEK Preprint No. 98-44, 1998.

[5] The maximum surface temperature of the cavity is about 60 degC during high-power operation.

[6] SuperKEKB design report, to be published as a KEK Report.

[7] T. Abe, T. Kageyama, H. Sakai, Y. Takeuchi, and K. Yoshino, in Proceedings of the 10th Annual Meeting of Particle Accelerator Society of Japan, August 2013 (Paper ID: SAP057).

[8] H. Sakai, et al., to be published as a KEK Internal Report.

[9] J. W. Wang and G. A. Loew, SLAC-PUB-7684, 1997.